VECTOR FIELD PATH PLANNING AND CONTROL OF AN AUTONOMOUS ROBOT IN A DYNAMIC ENVIRONMENT

*J.C. Wolf, P. Robinson, J.M. Davies**

School of Computing, Communications and Electronics,
*School of Mathematics and Statistics,
University of Plymouth,
Plymouth, PL4 8AA, Devon, U.K.

ABSTRACT

Potential field methods are discussed as possible solutions to obstacle avoidance for mobile robots. A new solution to well known problems associated with potential fields is presented. The design of a general control system, using frequency domain analysis of the input signal, that matches the path planning method to a robot's dynamics, is discussed. Preliminary experimental results are presented and suggestion for further work proposed.

1. INTRODUCTION

A variety of path planning methods for mobile robots have been developed over the past two decades [1-4,7]. The potential field method is one of the more popular methods used in robot path planning due to its mathematical simplicity, elegance and its suitability for dynamic environments. One of the original works on potential field methods is by Khatib [1], who applied the method to manipulators as well as mobile robots. Khatib describes the idea as follows:

"*The manipulator moves in a field of forces. The position to be reached is an attractive pole for the end effector and obstacles are repulsive surfaces for the manipulator parts.*"

This paper introduces a theory which tries to resolve the problems identified in [2] and [3] particularly with regard to the oscillation problems. One part of the theory involves an improvement in the path prediction and a second part of the theory involves making an improvement in the tracking error arising from the dynamics of the system.

2. POTENTIAL AND FORCE FIELD METHODS

Mobile robots and obstacles can be treated as single points provided their dimensions are small in comparison to the workspace. These points act as repulsive and attractive poles in a force field.

2.1. General Theory

Consider a 2 dimensional Cartesian coordinate system (x,y) in the plane of the football pitch, where x and y axes are along two perpendicular sides of the rectangular football pitch as shown in Figure 1.

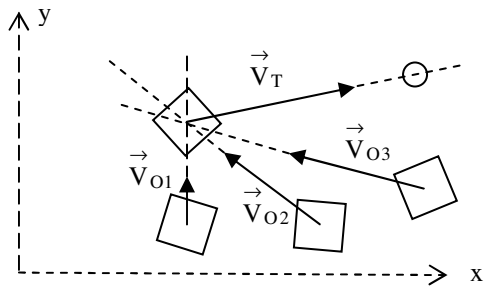

Figure 1. Diagram showing a controlled robot, 3 obstacles and a target position.

In general the resultant force acting on a controlled robot at any position in the force field can be expressed as the sum of repulsive forces from obstacles and the attractive force towards the target as shown in equation (1)

$$\vec{V}_p = \vec{V}_T + \frac{1}{n}\sum_{i=1}^{n}\vec{V}_{Oi} \qquad (1)$$

where n is the number of obstacles within a close range of the robot, $\vec{V}_{Oi}$, $i = 1..n$, are the repulsive forces acting on

the robot due to the i[th] obstacle, $\vec{V}_T$ is the attractive force towards the target and $\vec{V}_p$ is the resultant force acting on the robot.

It should be noted that the magnitudes of the repulsive forces are chosen to be dependant on the distances of the obstacle from the robot. However the magnitude of the target force can be set to a constant or set to a function of the distance of the target from the robot [1]. In our paper we have chosen the target force to be a constant.

Previously developed potential field methods have force vectors which originate in a direction perpendicular to an obstacle surface with a magnitude that reduces with increasing distance from the obstacle. This approach is similar to that used in electric or gravitational potential energy field theory. However, as pointed out by Y.Koren and J.Borenstein [2], this approach is too simplistic and these authors have identified the following main problems:

1. Trap situations due to local minima (cyclic behaviour)
2. No passage between closely spaced obstacles
3. Oscillations in the presence of obstacles
4. Oscillations in narrow passages

A further problem mentioned in [2] and also in [3] is that high speed robots deviate from the direction path of the force field. This is an important problem if robots are required to move at a high speed, as in the case of robot football. The root of the problem lies in that the robot dynamics cannot give rise to instantaneous path changes and therefore cannot follow the generated vector field. Some of these problems are associated with a speed restriction being required on paths which have a small radius of curvature.

2.2. The presented vector field theory

Most theories use equation (1) to compute the robot path which results in a path of minimum potential energy.
In the presented theory, a modification to equation (1) is proposed in which each obstacle repulsive force, $\vec{V}_{T90i}$, acts in a direction which is perpendicular to the target unit vector $\vec{V}_T$ as shown in Figure 2.
Equation (1) is now modified to give the resultant force acting on the robot and is given by

$$\vec{V}_p = \vec{V}_T + \frac{1}{n}\sum_{i=1}^{n} \vec{V}_{T90i} \qquad (2)$$

To simplify the notation only one obstacle will be considered where the repulsive force is denoted by $\vec{V}_{T90}$.

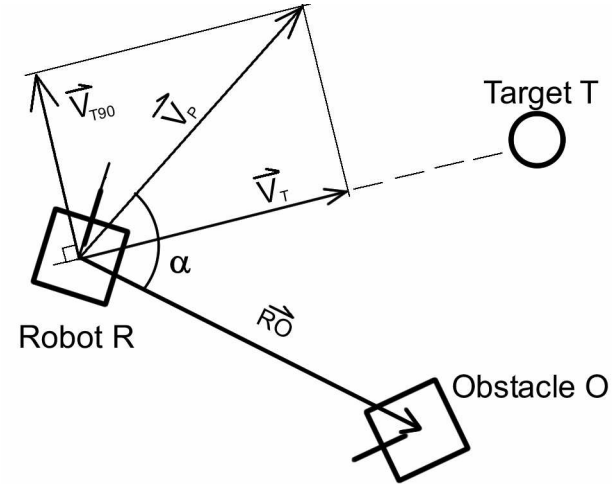

Figure 2. Vector field forces acting on controlled robot

Let $x = \left|\overrightarrow{RO}\right|$ represent the distance between the robot and the obstacle. Let α be the angle between vectors $\vec{RO}$ and $\overrightarrow{V_p}$ as shown in Figure 2.

The magnitude of $\vec{V}_{T90}$ is to be defined by the formula

$$\left|\overline{V}_{T90}\right| = k\,G_a(x,\mu,\sigma) \qquad (3)$$

where $G_a(x,\mu,\sigma) = e^{-\frac{(x-\mu(\alpha))^2}{2\sigma^2}}$ is a non-normalised Gaussian distribution function, $\mu(\alpha)$ is a mean length which is dependant on the angle α, σ^2 is a constant variance and k is a constant scaling factor.

A Gaussian distribution was chosen in this theory since this function gave a more gradual build up of the force as the robot approaches an obstacle. Some initial experiments, not described here, have shown that this function leads to better path stability, minimum oscillations and less tracking error when compared to other types of functions such as the force inverse power law.

The Gaussian function used in equation (3) has the property in which a maximum value occurs when the distance $x = \mu(\alpha)$ and has a zero value when x tends to infinity. For reasons further explained in section 2.3, a

function $\mu(\alpha)$ is introduced which is defined in equation (4). This function allows the robot path to be optimised after the robot has traversed a particular obstacle.

$$\mu(\alpha) = \frac{2r_l}{\left(1+e^{\alpha/\tau}\right)} \qquad (4)$$

where τ is a constant angle and r_l represents a maximum value for μ at an angle $\alpha = 0$. This function was suitably chosen to represent a monotonically decreasing function of α and to give rise to a strong influence on the path direction when α is small (i.e. when the robot is travelling towards the obstacle) and a negligible influence on the path direction when α becomes large (i.e. when the robot has traversed the obstacle). A plot of $\mu(\alpha)$ is shown in Figure 3 for the case when $r_l = 6$ and $\tau = 30°$.

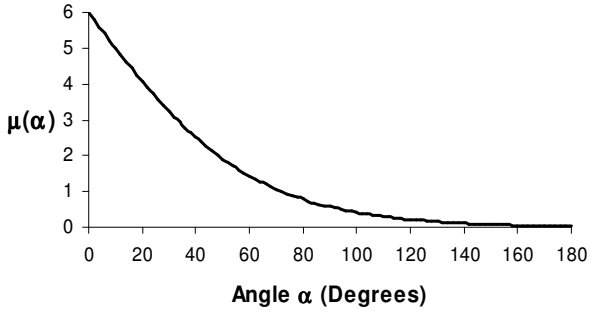

Figure 3. Plot of $\mu(\alpha)$ as a function of α

2.3 Calibration Procedure

For the case of the Gaussian distribution, a value of σ is chosen to give a reasonable magnitude of the repulsive force when $x = \mu + \sigma$. i.e. when x lies at one standard deviation away from the mean of the Guassian distribution. This calibration constant will be dependent on the dimensions of the obstacle.
For the function $\mu(\alpha)$, the constant τ is chosen to give an offset value of approximately $0.1r_l$ when $\alpha = 90^o$. This corresponds to a value of $\tau \approx 30^o$.

Figure 4 shows a typical path of the robot when an obstacle is placed between a start point and the target. In order to demonstrate the influence of the function $\mu(\alpha)$ on the robot the path for the case when $\mu = 0$ is also presented. It should be noted that different k values were used for the two paths so that both paths arrive at the same point in the workspace when the robot has begun to traverse the obstacle.

It can clearly be seen in Figure 4 that the robot does not follow the most direct route to the target, after traversing the object, unless the function $\mu(\alpha)$ is taken into account in the theory. The more direct route has less curvature and therefore the robot can attain a higher speed and therefore result in a lower approach time.

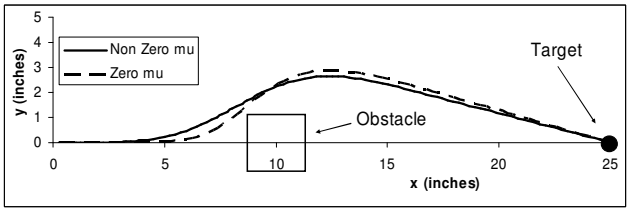

Figure 4. The path of a robot starting at (0,0) and avoiding an obstacle on the way to target at (25,0) with $\tau = 30°, \sigma = 2, r_l = 2$

The system described so far represents the Vector-field Generator block shown in Figure 5. A description of the remaining part of the complete block diagram appears in the following section.

3. PATH PLANNER

3.1. Control System

The desired heading angle of the robot at any point in the workspace is denoted by θ_{in} and is equal to the direction angle of the resultant force.

i.e. $\theta_{in} = \angle \vec{V}_p$ (5)

It should be noted that θ_{in} is the input to a control system that aligns the robot. However the magnitude of $\vec{V}_p$ is not used in the control system. In a complex dynamic environment with many obstacles, this input is somewhat unpredictable. Therefore the designed control system needs to lower the robot's speed to the required level in order for the control system to follow θ_{in} with minimum tracking error.

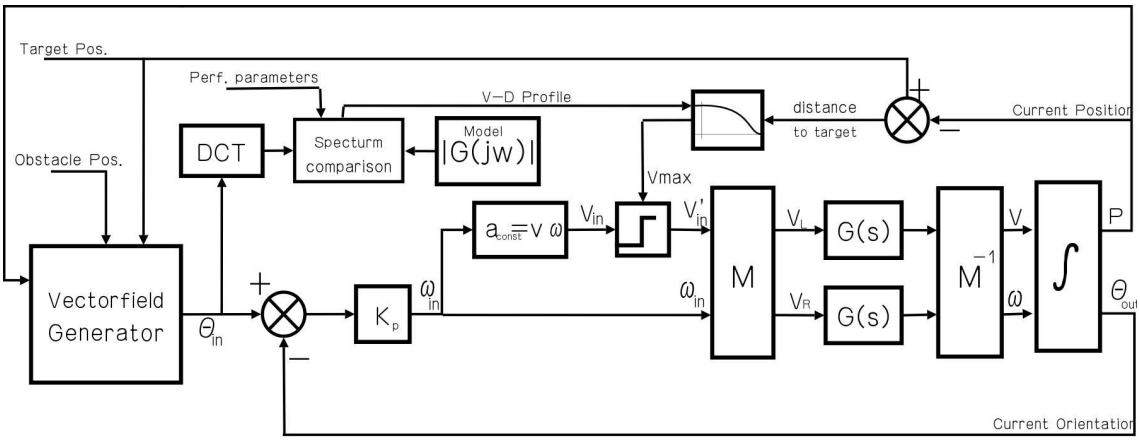

Figure 5. Complete block diagram of the Robot Control System

In order to detect a mismatch in the demanded trajectory to the robots capabilities, a simulation program executes the robots path before actual robot movement is set to take place. During this simulation period the controller input $\theta_{in}(t)$ is measured and stored into memory. The measured signal is then transformed into the frequency domain which provides information about the required bandwidth of the path. The transform is defined in equation (6).

$$\Theta_{in}(j\omega) = \mathcal{F}\{\theta_{in}(t)\} \tag{6}$$

where $\mathcal{F}$ denotes the Fourier transform.

By comparing $\Theta_{in}(j\omega)$ to the vehicle bandwidth $G(j\omega)$ it can be determined if the vehicle bandwidth is exceeded. In this case the demanded speed of the robot must be reduced.

The current heading angle of the robot is subtracted from the demanded heading angle generated to produce the angular velocity ω_{in}. The controller aims to continuously line up the robot with the vector-field. The magnitude of the forward velocity $V_{in}^{`}$ (defined in equation (8)) is also computed and is used as an input to the controller. To avoid skidding, e.g. as a result of a large centripetal force, the value of V_{in} must be constrained to an upper limit. (This upper limit is dependent upon a number of factors including the coefficient of friction of the tyres and robot mass). This ensures that the normal acceleration does not exceed a known limit. For circular motion, the inward acceleration is related to the angular velocity ω and the velocity v by the formula $a = v\omega$. On using this formula, V_{in} can be expressed as

$$V_{in} = \frac{a_{const}}{\omega_{in}} \tag{7}$$

The forward velocity is defined in equation (8).

$$V_{in}^{`} = \begin{cases} V_{max} & \text{if } V_{in} > V_{max} \\ V_{in} & \text{otherwise} \end{cases} \tag{8}$$

where V_{max} is a known maximum target approach velocity and is influenced by the path frequency spectrum error. For a two-wheel differential drive robot [6] the left hand and right hand robot wheel velocities $V_{L\,in}$ and $V_{R\,in}$ respectively are then computed using the formulas

$$\begin{bmatrix} V_{Lm} \\ V_{Rm} \end{bmatrix} = M \begin{bmatrix} V_{in}^{`} \\ \omega_{in} \end{bmatrix} \text{ where matrix } M = \begin{bmatrix} 1 & -L/2 \\ 1 & L/2 \end{bmatrix} \tag{9}$$

The transfer-function block G(s), which appears in Figure 5, relates the requested wheel velocity (input) to the current wheel velocity (output). This function represents the wheel velocity of the robot. A discrete version of G(s) is used in the simulation part of the path planning.

3.2 Robot Model

A real velocity-controlled robot football player can be modelled approximately by a first or second order linear system combined with a non-linear rate-limiter and a pure time delay. The time delay is due to the time required for radio transmission and vision system processing. The rate-limiter limits the acceleration of the robot since a real robot can only accelerate with a torque which is proportional to

the maximum current of the circuit. The robot acceleration is also limited in order to prevent forward wheel slip and to conserve battery power.
A block diagram of the real model is shown Figure 6 below.

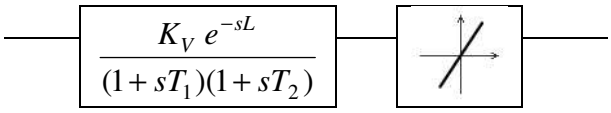

Figure 6. Real Model Block Diagram

In the SimuroSot Middle league simulator, the transfer function G(s) has been determined by a step response experiment and can be modelled by the transfer function

$$G(s) = \frac{K_V\, e^{-T_D s}}{1+T_1 s} \qquad (10)$$

where T_D is the delay in the simulator,
T_1 is the system time constant,
and K_V is an amplification factor

4. EXPERIMENTS AND RESULTS

In the limited time available it has not been possible to conduct a full range of experiments in order to test and verify the theory developed here. Notwithstanding these restrictions a series of practical tests have produced encouraging results.

4.1 Determination of Robot Models

The step response experiment, referred to in section 3.2, of the robot velocity at each time frame is shown in Figure 7.

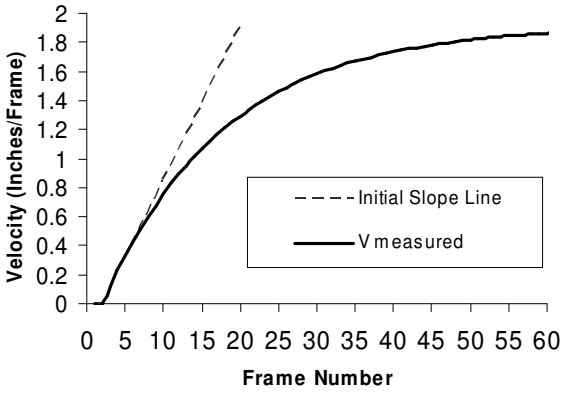

Figure 7. Step-response of a SimuroSot robot. Velocity unit in inches/frame. (fps = 60Hz)

The constants K_V , T_D, and T_1, required in equation (10), were obtained by curve fitting the data shown in Figure 7. The values of these constants are shown below.

T_D = 2 frames
T_1 = 16.7 samples
K_V = 1.88 to match the output to inches/frame.

The input range to the SimuroSot system has been scaled to lie in the range between -1 and 1. The transfer function G(s) is converted into a discrete transform G(z) with a sampling time being set to 1 frame.

The same step response experiment was carried out with a real robot football system as shown in Figure 8. Using curve fitting techniques, Figure 8 can therefore be used to determine the constants appearing in Figure 6.

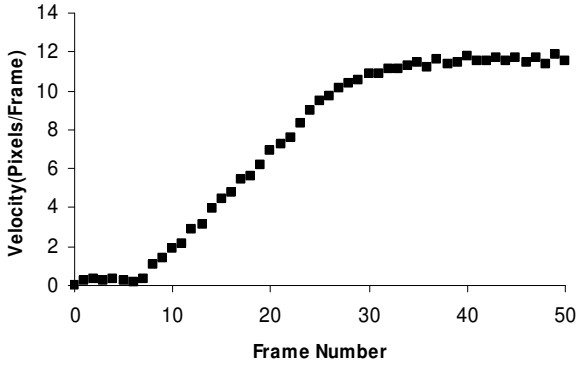

Figure 8. Step-response of a real football robot Velocity units in pixels/frame (frame-rate = 50Hz, 768 pixels to 2.2m) noting the large dead-time at the beginning from the frame grabber.

A comparison between the simulated path and the real robot path is shown in Figure 9. The difference between the two paths is due to the inaccuracy of the model used in equation (10). However the simulation is accurate enough to predict the arrival time.

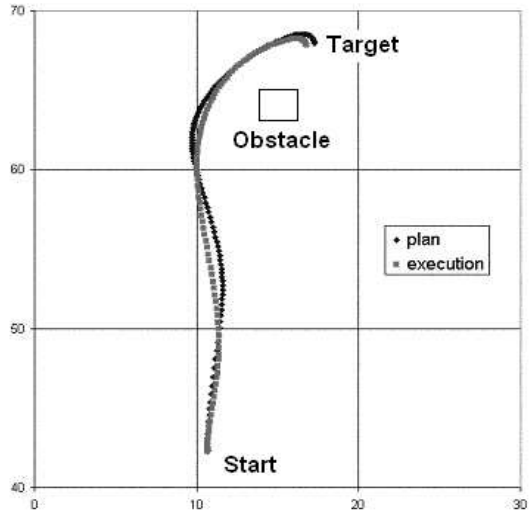

Figure 9. Comparison between the simulated path and the real executed path.

5. CONCLUSION

The disadvantages of traditional vector field navigation have been identified. A modification to vector field navigation, which improves robot navigation and obstacle avoidance behaviour, has been demonstrated. This new variation uses a repulsive force perpendicular to the target line of sight and characterised by a Gaussian distribution, to ensure collision is avoided. In this case, the robot is guided on a smooth path around the obstacle. This enables higher operational speeds to be achieved.

A generic controller which helps optimise the new vector field method has been designed. By comparing the bandwidth of the demand signal to the bandwidth of the robot, the controller ensures that over ambitious commands, e.g. a tight, high speed turn which would cause the robot to skid, are avoided. The controller is designed to automatically limit input commands so that they are within the dynamic capabilities of the robot. In the near future it is hoped to use a Mirosot robot to successfully demonstrate the new vector field method working in unison with the generic controller. Potential time delays during operation are identified as a possible source of concern.

6. REFERENCES

[1] Oussama Khatib, “Real-Time Obstacle Avoidance for Manipulator and Mobile Robots” The International Journal of Robotics Research, MIT Press, Cambridge USA, pp 90-98, Spring 1986

[2] Y. Koren, J. Borenstein, “Potential Field Methods and Their Inherent Limitations for Mobile Robot Navigation”, IEEE Conference on Robotics and Automation, Sacramento California, pp 1398-1404, April 1991

[3] Prahlad Vadakkepat, Tong Heng Lee and Liu Xin, “Application of Evolutionary Artificial Potential Field in Robot Soccer System”, National University of Singapore, Singapore 2001

[4] M. Khatib, R. Chatila, “An Extended Potential Field Approach for Mobile Robot Sensor-Based Motions”, Proceedings of the Intelligent Autonomous Systems IAS-4, IOS Press, Karlsruhe Germany, pp. 490-496,March 1995

[5] Man-Wook Han, Peter Kopacek, “Neural Networks for Control of soccer robots”, Institute for Handling Devices and Robotics, Vienna University of Technology, Vienna, Austria. Published in the ISIE’2000, Cholula, Puebla, Mexico

[6] Phillip J. McKerrow, “Introduction to Robotics”, Addison-Wessley, Sydney, Australia, pp. 402-420, 1991

[7] Roland Siegward, Illah R. Nourbakhsh, “Introduction to Autonomous Mobile Robots”, MIT Press, Cambridge, Massachusetts, London, England, pp. 267-272, 2004